Extensive dissolution of live pteropods in the Southern Ocean

Bednaršek N[1], Tarling GA[1]*, Bakker DCE[2], Fielding S[1], Jones EM[3], Venables HJ[1], Ward P[1], Kuzirian A[4], Lézé B[2], Feely RA[5], Murphy EJ[1]

*corresponding author: gant@bas.ac.uk

1. British Antarctic Survey, Natural Environment Research Council, Madingley Rd, Cambridge, CB3 0ET, UK
2. School of Environmental Sciences, University of East Anglia, Norwich Research Park, Norwich NR4 7TJ, UK
3. Royal Netherlands Institute for Sea Research, P.O. Box 59, 1790 AB Den Burg, Texel, The Netherlands
4. Department of Geology and Geophysics, Woods Hole Oceanographic Institution, Woods Hole, Massachusetts, USA
5. NOAA, Pacific Marine Environm Lab, Seattle, WA 98115 USA

Extensive dissolution of live pteropods in the Southern Ocean

Bednaršek N[1], Tarling GA[1]*, Bakker DCE[2], Fielding S[1], Jones EM[3], Venables HJ[1], Ward P[1], Kuzirian A[4], Lézé B[2], Feely RA[5], Murphy EJ[1]

*corresponding author: gant@bas.ac.uk

1. British Antarctic Survey, Natural Environment Research Council, High Cross, Madingley Rd, Cambridge, CB3 0ET, UK

2. School of Environmental Sciences, University of East Anglia, Norwich Research Park, Norwich NR4 7TJ, UK

3. Royal Netherlands Institute for Sea Research, P.O. Box 59, 1790 AB Den Burg, Texel, The Netherlands

4. Department of Geology and Geophysics, Woods Hole Oceanographic Institution, Woods Hole, Massachusetts, USA

5. NOAA, Pacific Marine Environm Lab, Seattle, WA 98115 USA

The carbonate chemistry of the surface ocean is rapidly changing as a result of human activities[1]. In the Southern Ocean, aragonite (a metastable form of calcium carbonate with rapid dissolution kinetics) may become undersaturated ($\Omega_A < 1$) in the upper layers by 2050[2]. This places at risk aragonite-shelled organisms such as euthecosome pteropods, which can dominate surface water communities in polar regions[3]. We provide field evidence that Southern Ocean pteropods are already showing signs of dissolution. Conditions where $\Omega_A \approx 1$, caused by mixing of upwelled deep-water with surface water containing anthropogenic CO_2, were found within 200 m of the surface. We extracted live specimens of the pteropod *Limacina helicina antarctica* from these undersaturated surface waters, as well as from supersaturated regions elsewhere, and compared their shell structure under SEM. Laboratory

incubations with a range of Ω_A saturation levels were carried out for up to 14 d.
Severe levels of shell dissolution were observed in the undersaturated region but
not elsewhere. 8 days of incubation in Ω_A 0.94-1.12 produced similar levels of
dissolution. Both deep-water upwelling and CO_2 absorption by surface waters is
likely to increase as a result of human activities[2,4], making upper ocean regions
where aragonite is undersaturated more widespread.

Aragonite skeletons and tests are important components of the oceanic carbon system
because they contribute a significant fraction of the global flux of particulate calcium
carbonate ($CaCO_3$) settling to the ocean floor[5]. They are especially important in the
short term buffering of the ocean absorption of anthropogenic CO_2[6, 7]. The surface
ocean is generally saturated with respect to aragonite ($\Omega_A > 1$) but the level of
saturation decreases with depth. The point at which Ω_A falls below 1 is called the
saturation horizon, and this generally occurs around 1000 m but has shoaled by
between 40 and 200 m as a direct consequence of the uptake of anthropogenic CO_2[2,8].
Dissolution of shelled organisms mainly occurs when Ω falls below 1 but it has also
been found in pteropods incubated in conditions where Ω_A was ≈ 1[9,10].

There are already reports of surface waters occasionally being undersaturated with
respect to aragonite, including those of the Arctic Basin in 2008 after extensive
melting of sea-ice[11] and along the California continental shelf after seasonal upwelling
of deep-water[1]. South of the polar front in the Southern Ocean, winter cooling and
strong persistent winds are believed to be responsible for the ventilation of deeper
waters to the surface, resulting in a natural decrease of carbonate ions of
approximately 25% (35 µmol/kg) relative to summer[12]. When combined with

52   increases in anthropogenic CO_2, ocean models predict that the Southern Ocean will

53   begin to experience widespread aragonite undersaturation in surface waters after the

54   year 2050[2,13].

55

56   Euthecosome pteropods are amongst a small number of taxa that make their shells

57   principally from aragonite. The effects of Ω_A undersaturation on pteropods have

58   mainly been investigated by laboratory incubations under enhanced partial pressures

59   of CO_2 (pCO_2), simulating future atmospheric CO_2 scenarios. Pteropods have been

60   found to exhibit shell malformations[14], lower rates of $CaCO_3$ precipitation[15] and

61   dissolution of the shell exterior[2]. Effects have also been described on dead specimens

62   collected in deep sediment traps[16], where shells exposed to aragonite undersaturation

63   had an opaque and pitted appearance. Byrne et al.[9] demonstrated that sinking dead

64   pteropods dissolved rapidly as they dropped below the saturation horizon. Feely et

65   al.[10] further found that dissolution in dead specimens starts at Ω_A levels at or just

66   below 1 across a range of North Pacific pteropod communities. Until the present

67   study, such effects have not been documented on live animals extracted directly from

68   the natural environment.

69

70   Sampling was carried out in the Scotia Sea, located in the Atlantic Sector of the

71   Southern Ocean, where the strong flow of the Antarctic Circumpolar Current (ACC)

72   is constricted in width. It is a physically dynamic region where deep water upwelling

73   occurs[17] and eddies from frontal regions are frequently encountered[18]. The interaction

74   of strong ACC flows coupled with bottom topography leads to greater micronutrient

75   availability and hence extensive phytoplankton blooms downstream of topographic

76   features[19,20].

77

Live pteropods from this region were collected in January and February 2008 during

cruise JR177 on RRS *James Clark Ross* as part of the British Antarctic Survey

Discovery 2010 program. Water sampling and depth-discrete net-catches of

mesozooplankton to 400 m were done along a south to north transect within the Scotia

Sea (Fig. 1). The saturation horizon for aragonite was 1000 m across the majority of

the transect. However, at station Su9 (52.6ºS, 39.1ºW), there was a notable incursion

of waters with low Ω_A values (minimum of 0.997) into layers above 400 m (Fig. 2).

85

Limacina helicina antarctica dominates mesozooplankton biomass in a number of

Southern Ocean regions where it is the principle calcifying organism[21]. It is most

commonly found above 400 m depth, particularly concentrating in the layers between

200 m and the surface[3]. It has life-cycle that can last upwards of 2 years, in which

time it grows to 1 cm in shell diameter[21]. Analysis was carried out on both freshly

caught material preserved directly upon collection and on specimens that were

incubated under manipulated CO_2 levels (375 to 750 parts per million at 4°C) in order

to establish a response index. All freshly-caught and incubated specimens were

preserved in 70% ethanol. Subsequently, they were treated to dehydrate shell-layers

and to remove the periostracum (Fig. 3) so that the state of the underlying shell matrix

could be examined using SEM.

97

Different degrees of dissolution were identified in incubated shells of live pteropods

(see supplementary information). We categorised them into three main levels

according to the degree of encroachment upon the upper prismatic layer and into the

upper shell layer (Fig. 4). Specimens were scored blind and then correlated back to

4

102   the experimental conditions. Incubations in which even only a slight degree of

103   undersaturation was experienced for 8 d (Ω_A 0.94-1.12, pCO_2 of 675 µatm) was

104   sufficient to cause substantial dissolution of the shell matrix relative to the

105   supersaturated control (Ω_A 1.62-1.78, Fig. 5). We then examined freshly caught

106   material, preserved directly upon collection, for signs of such shell dissolution.

107

108   *L. helicina antarctica* juveniles were found at all sampling stations, with northern

109   stations (<57ºS) containing higher abundances (7.2 x 10^4 to 3.4 x 10^4 ind. m^{-2}) than

110   those to the south (>57ºS; 2.9 x 10^2 to 1.9 x 10^3 ind. m^{-2}). At station Su9, we found *L.*

111   *helicina antarctica* juvenile specimens contained all three levels of dissolution.

112   Juveniles from other stations only contained small patches of the least severe level of

113   dissolution (Figs. 2, 5), probably caused by Ω_A-undersaturated microenvironments

114   close to the exterior surface resulting from the remineralisation of organic matter[22].

115

116   Dissolution of live specimens from Su9 was apparent over the entirety of their shells

117   as opposed to just the inner whorls or the growing edge. This indicates firstly that the

118   periostracum (the outer organic layer) provides little if any protection to the

119   underlying shell matrix. If it did so, then parts where the periostracum is thinnest, e.g.

120   at the growing edge, would have been more affected. Secondly, dissolution must have

121   occurred recently, else it would have only been apparent on the oldest, inner whorls

122   and not at the newly deposited growing parts of the shells. We conclude that the

123   observed dissolution was principally a physico-chemical response to the carbonate

124   chemistry conditions in a body of water inhabited for the last 4 to 14 d. The

125   dissolution response is similar to that found in dead specimens incubated at $\Omega_A \approx 1$

126   reported by Byrne et al.[9] and Feely et al.[10] underlining the fact that live specimens

127 have little to protect themselves from the effects of Ω_A undersaturation. Furthermore,

128 in both live and dead specimens, it is apparent that dissolution can occur rapidly even

129 when in just close proximity to the aragonite saturation horizon.

130

131 Regions of upwelling that bring the saturation horizon close to the surface are likely

132 to be repeated through much of the Southern Ocean and are not a modern

133 phenomenon[12]. These deep-waters probably came into contact with the atmosphere

134 around 1000 years ago and so are unlikely to contain any anthropogenic CO_2. Mixing

135 with surface waters will normally increase Ω_A to above saturation levels but increases

136 in surface concentrations of CO_2 will reduce the effect of this dilution. At station Su9,

137 an Ω_A of around 1 was observed up to a depth of about 200 m despite mixing with

138 surface water. Calculations of the effect of anthropogenic carbon mixing down from

139 surface waters (see supplementary information) showed a reduction of Ω_A values of

140 approximately 0.1 relative to pre-industrial values. Station Su9 was a site of

141 comparatively high phytoplankton biomass (60 to 90 mg C m^{-3})[20]. However DIC

142 levels below 100 m were similar to another site with similar water mass properties but

143 low phytoplankton biomass[20], indicating that extensive remineralization had not taken

144 place and the carbon export had not significantly lowered values of Ω_A. Therefore, the

145 primary causes of low Ω_A values observed in this instance were mainly from the

146 addition of anthropogenic CO_2 in surface waters mixing with upwelled deep-water.

147

148 Climate models project a continued intensification in Southern Ocean winds

149 throughout the 21st century if atmospheric CO_2 continues to increase[4]. In turn, this

150 will increase wind-driven upwelling and potentially make instances of deep-water,

151 under-saturated in aragonite penetrating into the upper mixed layers more frequent.

152   Simultaneously, rising atmospheric concentrations of anthropogenic CO_2 will

153   continue to reduce aragonite saturation levels in surface waters, particularly in polar

154   regions[12]. Conditions such as observed at station Su9 are therefore likely to become

155   more common in the Southern Ocean, making shell-dissolution an increasing threat to

156   pteropod populations.

157

158   Pteropods do not necessarily die as a result of dissolution. Calcification of the inside

159   of the shell probably continues and, to some degree, counteracts the dissolution of the

160   exterior of the shell. Nevertheless, the observed rapidity of the dissolution response

161   means that, in the present instance, there would have been net loss of shell overall, as

162   reported in other experimental manipulations[15]. The main consequence of such loss of

163   shell is an increased vulnerability to predation and infection, which will in turn impact

164   other parts of the foodweb[15]. A drop in their population size will affect the ocean's

165   carbonate cycle given the important role of pteropods in balancing oceanic alkalinity

166   budgets[7]. Rates of vertical carbon flux will also decline, as the pteropod shells

167   become less dense and less able to act as ballast for other particulate material[23].

168

169   This report documents a dissolution response of live pteropods within their natural

170   environment as a result of exposure to waters where $\Omega_A \approx 1$. The data validate the

171   prediction of a wide body of laboratory-based studies on the vulnerability of this

172   important taxon to the acidification of polar oceans[2,14,24]. The shallow aragonite

173   saturation horizon we observed was at least partially the result of oceanic absorption

174   of anthropogenic CO_2 and demonstrates that the impact of ocean acidification is

175   already occurring in oceanic populations, long before some projected dates of Ω_A

176   undersaturation[12]. Regional declines of pteropods populations may occur sooner than

177 presently projected as areas of Ω_A undersaturation in Southern Ocean surface waters

178 become more widespread.

179

180 **Methods**

181 *Field sampling*: Samples were collected along a south to north transect within the

182 Scotia Sea region of the Southern Ocean (60°S and 48°W to 50°S 34°W, Fig. 1) in

183 February 2008 on board the *RRS James Clark Ross*. Full-depth CTD casts and

184 plankton net samples were collected every 60 to 100 km along the transect. Water

185 samples were collected every 50 m down to 200 m depth and then every 200 m down

186 to 1000 m depth during each CTD cast. Juvenile *L. helicina antarctica* were collected

187 in the upper water column (0-400 m) with a vertically hauled motion compensated

188 Bongo net (0.5m^2, 100 µm and 200 µm meshed nets). Captured specimens were either

189 preserved immediately in 70% ethanol or used in incubation analyses.

190

191 *Water analysis*: Water samples were used for dissolved inorganic carbon (DIC) and

192 total alkalinity (TA) analysis following the Standard Operating Procedures for oceanic

193 CO_2 measurements (30), detailed in Jones et al.[20]. A VINDTA (Versatile INstrument

194 for the Determination of Titration Alkalinity, Marianda, Kiel, Germany) was used to

195 measure DIC and TA, with a Certified Reference Material (CRM) analysed in

196 duplicate for DIC and TA at the beginning and end of each sample analysis day. The

197 concentration of DIC was determined using the principles of coulometric analysis[25].

198 The accuracy of the DIC measurements was 2.4 µmol kg^{-1} and the precision, 1.5 µmol

199 kg^{-1}. Analysis for TA was carried out by potentiometric titration with hydrochloric

200 acid to the carbonic acid end point[26]. The accuracy and precision of TA values was

201 2.6 µmol kg^{-1} and 1.0 µmol kg^{-1} respectively.

202

203   DIC and TA, alongside temperature, salinity, pressure and macronutrient

204   concentrations from all discrete samples, were used to calculate the remaining

205   carbonate chemistry parameters including total pH (pH_T) and Ω aragonite (Ω_A). This

206   was done using the CO_2Sys programme[27] with thermodynamic dissociation constants

207   for K_1 and K_2 by Mehrbach et al.[28] and the re-fit by Dickson and Millero[29].

208

209   *Pteropod analysis*: Before further analysis, captured pteropod specimens were

210   inspected to select only those that had not suffered mechanical damage during

211   capture. Two sets of control samples were taken to consider capture and incubation

212   effects – one immediately fixed post capture from an Ω_A supersaturated region

213   (natural control), another after varying lengths of incubation in Ω_A supersaturated

214   conditions ($\Omega=1.7\pm0.08$; incubation control). There was no evidence of the more

215   advanced stages of dissolution (levels II and III) in either the natural or incubation

216   control samples. Level I dissolution covered just under 10% of the surface area in the

217   natural control sample, and 56% of surface area in the incubation control, indicating

218   an incubation effect. Accordingly, dissolution levels II and III were given most weight

219   as indicators of dissolution when comparing incubated material with that taken

220   directly from the natural environment.

221

222   Incubations were carried out in 0.22 GF/F filtered seawater to remove bacteria and

223   held in 2 L blacked-out flasks through which was bubbled synthetic air containing one

224   of four different CO_2 mixing ratios (xCO_2) (BOC Special Products): 375, 500, 750

225   and 1200 ppm ($\mu mol/mol$). Bubbling was stopped once water reached the correct CO_2

226   mixing ratio and around 50 individuals (principally juveniles) were introduced to the

227 flask, which was subsequently sealed, with head space kept to a minimum.

228 Incubations were run for between 4 and 14 d, with water samples taken at the start

229 and end of each incubation to verify Ω_A state (as above). Accordingly, each flask was

230 categorised into one of three Ω_A states: supersaturated (1.1 to 1.8), transitional (0.95-

231 1.1) or under-saturated (0.75 to 0.95). All pteropods were preserved in 70% ethanol.

232

233 Preserved pteropod shells were prepared as detailed in Bednarsek et al.[30]. Firstly,

234 abiogenic crystal precipitates on the shell surface were removed with 6% hydrogen

235 peroxide (H_2O_2), followed by a dehydration method including the use of 2,2-

236 dimethoxypropane (DMP) and 1,1,1,3,3,3-hexamethyldisilazane (HMDS). This

237 procedure was finely tuned to remove the precipitates without damaging any shell

238 layers. The overlying organic layer was then etched to expose the shell microstructure

239 for SEM analysis, using a JEOL JSM 5900LV at an acceleration voltage of 15kV and

240 a working distance of about 10 mm. 15 to 20 SEM photographs were taken across the

241 shell surface area of each specimen in order to determine the proportion of the shell

242 surface covered by each level of dissolution. Each image was analysed using

243 customised image-segmentation software (EDISON software) which estimated the

244 extent of each dissolution level in each image. Images were combined to determine

245 overall coverage for each specimen. Detailed description and user-guidelines on the

246 procedure are given at

247 http://coewww.rutgers.edu/riul/research/code/EDISON/index.html.

248

262

Author contributions

264   G.A.T and D.C.E.B. conceived the project; N.B. carried out the fieldwork, with the

265   assistance of G.A.T., S.F. and P.W.; E.M.J. and H.J.V. provided supporting

266   environmental data; A.K. helped develop a method of shell preparation for SEM

267   analysis; B.L. developed an image analysis method; G.A.T., N.B. and D.C.E.B co-

268   wrote the manuscript, with theoretical overviews provided by R.A.F. and all

269   remaining authors commenting.

270

Additional information

276

277

278 **References**

279   1.   Feely, R.A., Sabine, C.L., Hernandez-Ayon, J.M., Ianson, D. & Hales, B.

280   Evidence for upwelling of corrosive "acidified" water onto the continental

281   shelf. *Science* **320**, 1490-1492 (2008).

282   2.   Orr, J.C. *et al.* Anthropogenic ocean acidification over the twenty-first century

283   and its impact on calcifying organisms. *Nature* **437**, 681-686 (2005).

284   3.   Hunt, B.P.V. *et al.* Pteropods in Southern Ocean ecosystems. *Prog. Oceanogr.*

285   **78**, 193-221 (2008).

286   4.   Le Quere, C. *et al.* Saturation of the Southern Ocean CO2 sink due to recent

287   climate change. *Science* **316**, 1735-1738 (2007).

288   5.   Fabry, V.J. Shell growth rates of pteropod and heteropod molluscs and

289   aragonite production in the open ocean: implications for the marine carbonate

290   system. *J. Mar. Res.* **48**, 209-222 (1990).

291   6.   Broecker, W.S. & Takahashi, T. Neutralization of fossil fuel carbon dioxide

292   by marine calcium carbonate. in *The fate of fossil fuel CO_2 in the oceans* (eds.

293   Andersen, N.R. & Malahoff, A.) 213-241 (1977).

294   7.   Betzer, P.R. *et al.* The oceanic carbonate system - a reassessment of biogenic

295   control. *Science* **226**, 1074-1077 (1984).

296   8.   Feely, R.A. *et al.* Impact of anthropogenic CO_2 on the $CaCO_3$ system in the

297   oceans. *Science* **305**, 362-366 (2004).

298   9.   Byrne, R.H., Acker, J.G., Betzer, P.R., Feely, R.A. & Cates, M.H. Water

299   column dissolution of aragonite in the Pacific Ocean. *Nature* **312**, 321-326

300   (1984).

301 10.   Feely, R.A. *et al.* Winter-summer variations of calcite and aragonite saturation

302   in the Northeast Pacific. *Mar. Chem.* **25**, 227-241 (1988).

303   11.   Yamamoto-Kawai, M., McLaughlin, F.A., Carmack, E.C., Nishino, S. &

304   Shimada, K. Aragonite undersaturation in the Arctic Ocean: Effects of ocean

305   acidification and sea ice melt. *Science* **326**, 1098-1100 (2009).

306   12.   McNeil, B.I. & Matear, R.J. Southern Ocean acidification: A tipping point at

307   450 ppm atmospheric CO_2. *P. Natl. Acad. Sci. USA* **105**, 18860-18864 (2008).

308   13.   Steinacher, M., Joos, F., Frolicher, T.L., Plattner, G.K. & Doney, S.C.

309   Imminent ocean acidification in the Arctic projected with the NCAR global

310   coupled carbon cycle-climate model. *Biogeosciences* **6**, 515-533 (2009).

311   14.   Comeau, S., Jeffree, R., Teyssie, J.L. & Gattuso, J.P. Response of the Arctic

312   pteropod *Limacina helicina* to projected future environmental conditions. *Plos*

313   *One* **5**(2010).

314   15.   Comeau, S., Gorsky, G., Alliouane, S. & Gattuso, J.P. Larvae of the pteropod

315   *Cavolinia inflexa* exposed to aragonite undersaturation are viable but shell-

316   less. *Mar. Biol.* **157**, 2341-2345 (2010).

317   16.   Roberts, D. *et al.* Interannual pteropod variability in sediment traps deployed

318   above and below the aragonite saturation horizon in the Sub-Antarctic

319   Southern Ocean. *Polar Biol.* **34**, 1739-1750 (2011).

320   17.   Heywood, K.J., Garabato, A.C.N. & Stevens, D.P. High mixing rates in the

321   abyssal Southern Ocean. *Nature* **415**, 1011-1014 (2002).

322   18.   Kahru, M., Mitchell, B.G., Gille, S.T., Hewes, C.D. & Holm-Hansen, O.

323   Eddies enhance biological production in the Weddell-Scotia confluence of the

324   Southern Ocean. *Geophys. Res. Lett.* **34**, L14603. DOI:

325   10.1029/2007GL030430. (2007).

326   19.   Park, J., Ohb, I.-S., Kim, H.-C. & Yoo, S. Variability of SeaWiFs chlorophyll-

327   a in the southwest Atlantic sector of the Southern Ocean: Strong topographic

328   effects and weak seasonality. *Deep-Sea Res Pt. I* **57**, 604–620 (2010).

329   20.   Jones, E., Bakker, D., Venables, H. & Watson, A. Dynamic seasonal cycling

330   of inorganic carbon downstream of South Georgia, Southern Ocean. *Deep-Sea*

331   *Res. Pt. II*, doi: 10.1016/j.dsr2.2011.08.001 (2012).

332   21.   Bednarsek, N., Tarling, G., Fielding, S. & Bakker, D. Population dynamics

333   and biogeochemical significance of *Limacina helicina antartica* in the Scotia

334   Sea (Southern Ocean). *Deep-Sea Res. Pt. II* **59-60**, 105–116 (2012).

335   22.   Jansen, H., Zeebe, R.E. & Wolf-Gladrow, D.A. Modeling the dissolution of

336   settling $CaCO_3$ in the ocean. *Global Biogeochem. Cycles* **16**(2002).

337   23.   Francois, R., Honjo, S., Krishfield, R. & Manganini, S. Factors controlling the

338   flux of organic carbon to the bathypelagic zone of the ocean. *Glob.*

339   *Biogeochem. Cycles* **16**(2002).

340   24.   Fabry, V.J., McClintock, J.B., Mathis, J.T. & Grebmeier, J.M. Ocean

341   acidification at high latitudes: the bellweather. *Oceanography* **22**, 160-171

342   (2009).

343   25.   Johnson, K.M., Sieburth, J.M., Williams, P.J.L. & Brandstrom, L.

344   Coulometric total carbon dioxide analysis for marine studies - automation and

345   calibration. *Mar. Chem.* **21**, 117-133 (1987).

346   26.   Dickson, A.G. An exact definition of total alkalinity and a procedure for the

347   estimation of alkalinity and total inorganic carbon from titration data. *Deep-*

348   *Sea Res.* **28**, 609-623 (1981).

349   27.   Lewis, E. & Wallace, D.W.R. CO2SYS-Program developed for the CO2

350   system calculations. in *Carbon Dioxide Information and Analysis Centre.*

351   *Report ORNL/CDIAC-105.* (1998).

352   28.   Mehrbach, C., Culberson, C.H., Hawley, J.E. & Pytkowicz, R.M.

353   Measurement of the apparent dissociation constants of carbonic acid in

354   seawater at atmospheric pressure *Limnol. Oceanogr.* **18**, 897-907 (1973).

355   29.   Dickson, A.G. & Millero, F.J. A comparison of the equilibrium constants for

356   the dissociation of carbonic acid in seawater media. . *Deep-Sea Res.* **34**(1987).

357   30.   Bednarsek, N. *et al.* Description and quantification of pteropod shell

358   dissolution: a sensitive bioindicator of ocean acidification. *Global Change*

359   *Biol.* **18**, 2378-2388 (2012).

360

Figure Legends

362 **Figure 1: Scotia Sea showing sampling station positions and frontal positions at**

363 **time of sampling.** Dynamic height contours were used to determine the location of

364 the following fronts: *SB* Southern Boundary, *SACCF* Southern Antarctic Circumpolar

365 Current Front, south and north edge of Polar Front (S-PF, N-PF). 15% ice cover

366 represented by blue shading.

367

368 **Figure 2: Vertical profiles of Ω_A across the Scotia Sea (upper) and corresponding**

369 **dissolution levels in live juvenile *Limacina helicina antartica* (lower).** N is the

370 number of individuals analysed per station. Horizontal bars denote mean proportional

371 shell area per dissolution level across all specimens, error bars represent 1 SD. Level I

372 dissolution was significantly higher in Su9 specimens compared to all other stations

373 (Mann-Whitney rank sum test, T = 778, 20 and 35 df, P <0.001). Su9 was also the

374 only station in which level II and III dissolution was observed.

375

376 **Figure 3: SEM section of the shell of *Limacina helicina antartica*** showing the

377 organic layer (periostracum), prismatic layer and crossed-lamellar matrix of aragonite

378 crystals.

379

380 **Figure 4: SEM images of juvenile *Limacina helicina antarctica* (from which the**

381 **periostracum has been removed) showing different levels of dissolution.** (a,b)

382 intact animal without any indications of dissolution; (c) level I: the upper prismatic

383 layer slightly dissolved and the aragonite crystals of the crossed-lamellar matrix

384 starting to become exposed; (d) level II: the prismatic layer partially or completely

385 missing and the cross-lamellar matrix almost completely exposed; (e,f) level III: the

386   crossed-lamellar matrix showing signs of dissolution across large areas of the shell,

387   the shell becoming more porous [High resolution images are available in

388   Supplementary Information].

389

390   **Figure 5: Average (SD) proportion of different dissolution levels in live juvenile**

391   ***Limacina helicina antarctica* from the natural environment and ship-board**

392   **incubations.** Supersaturated refers to Ω_A >1.1, transitional, 0.95-1.1 and

393   undersaturated, 0.75 to 0.95. N refers to numbers of specimens analysed. Vertical bars

394   denote mean proportional shell area per dissolution level, error bars represent 1 SD.

395   14 d incubations in undersaturated conditions caused a significant increase in level III

396   dissolution compared to all other groupings (Kruskal-Wallis 1-way ANOVA, H =

397   51.7, 4 df, P <0.001). Amounts of level II and III dissolution were statistically

398   indistinguishable between Su9 and 8 d transitional incubations.

max. net
sampling depth

Depth

Su3　Su4　Su5　Su7　Su8　Su9

Dissolution level

No damage
level I
level II
level III

N = 8　N = 8　N = 3　N = 11　N = 5　N = 20

Proportion of shell area

Figure 3

Organic layer

Crossed-lamellar matrix

Prismatic layer
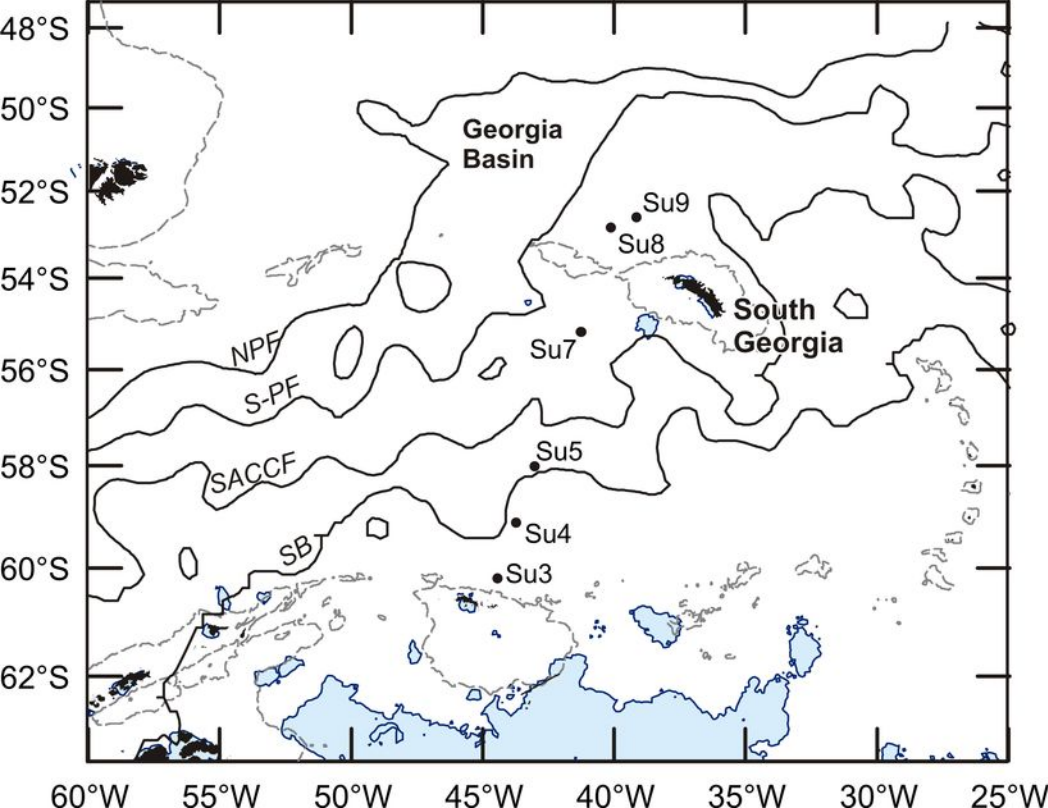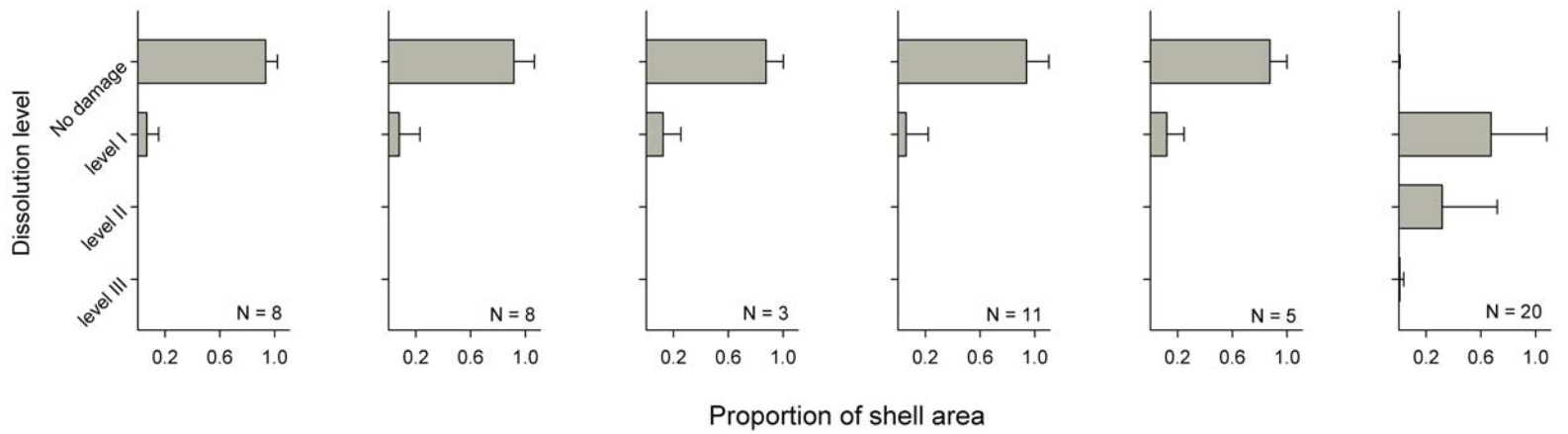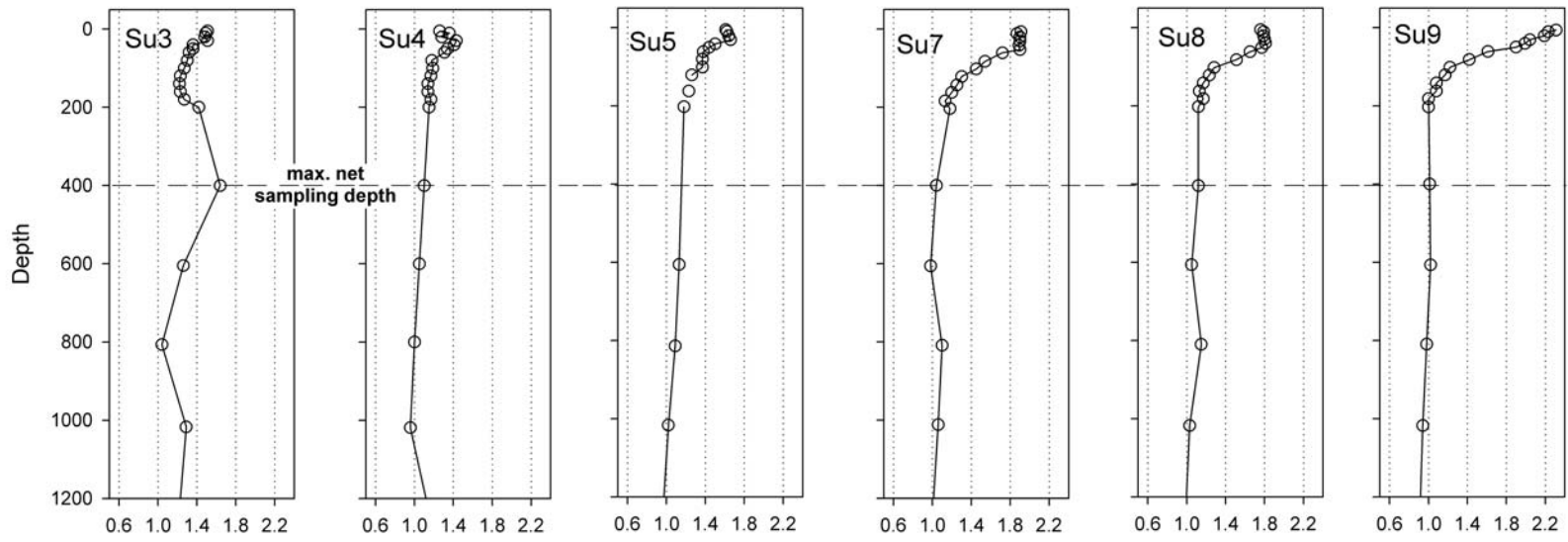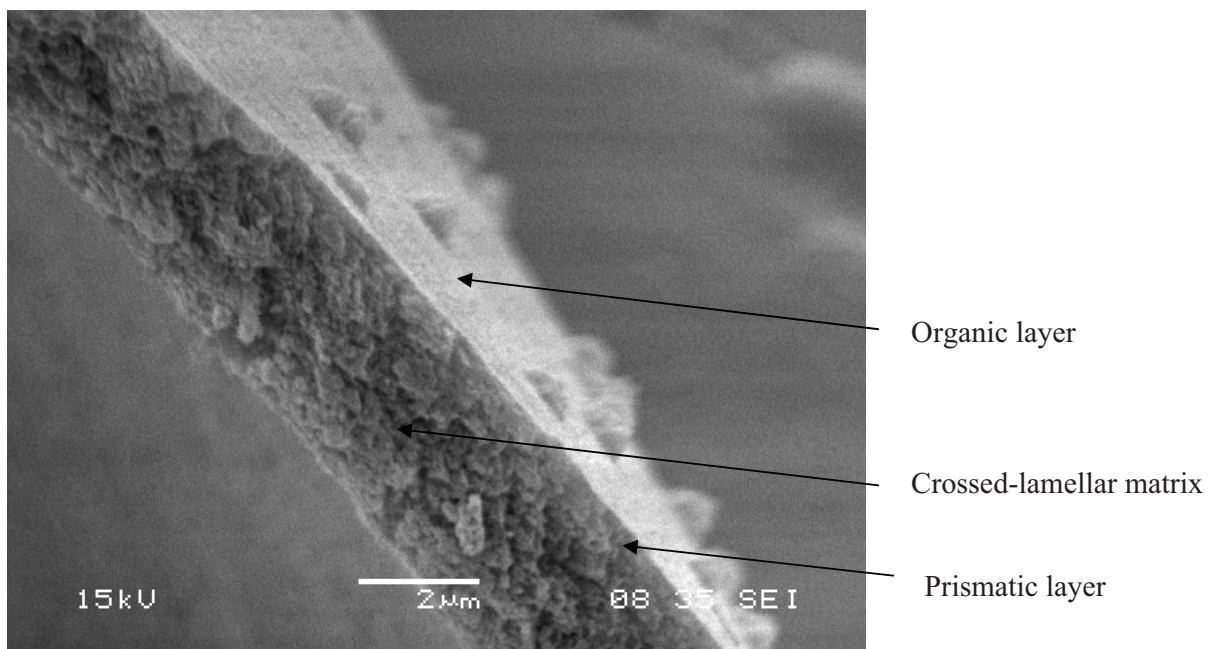
Figure 4
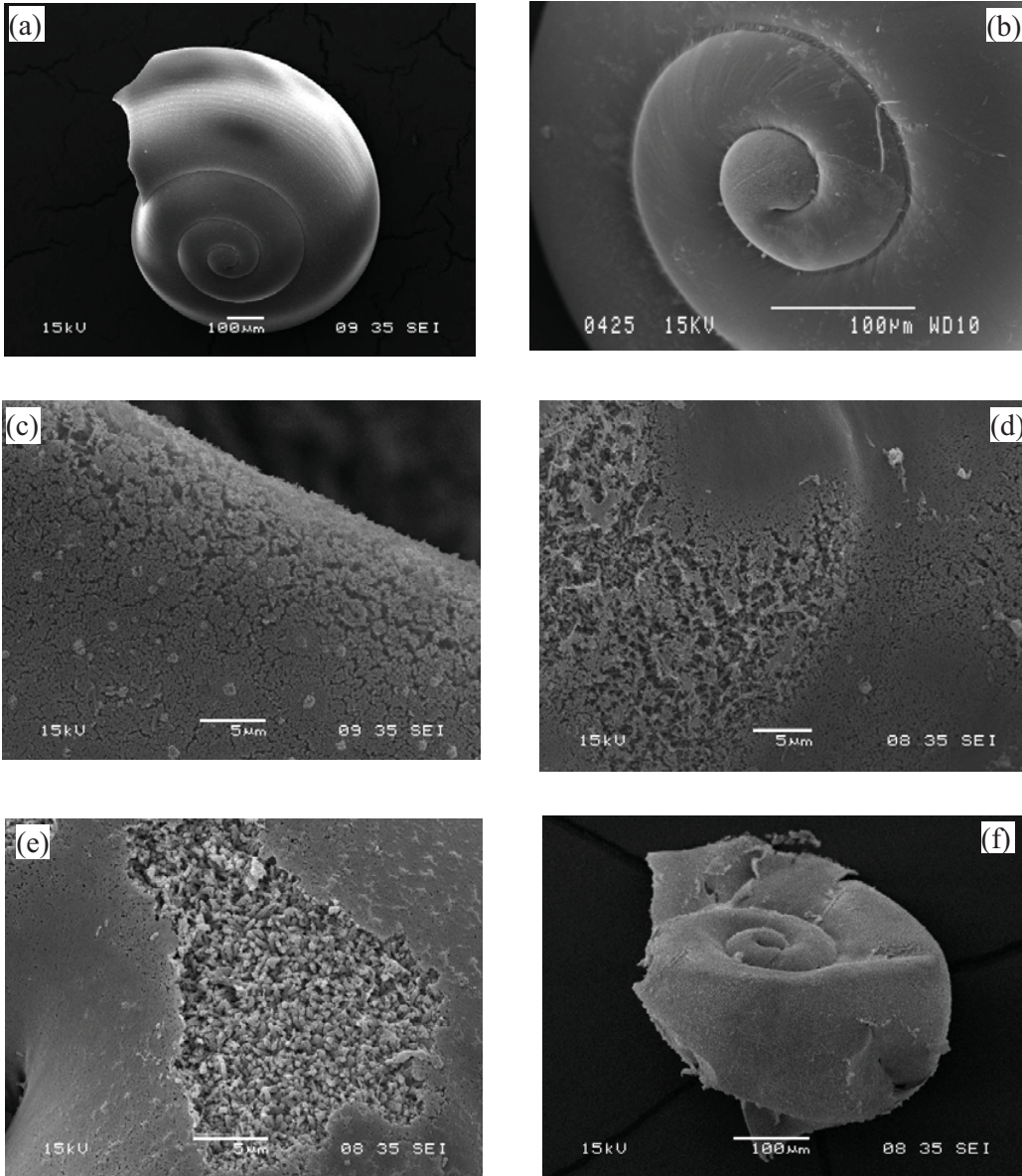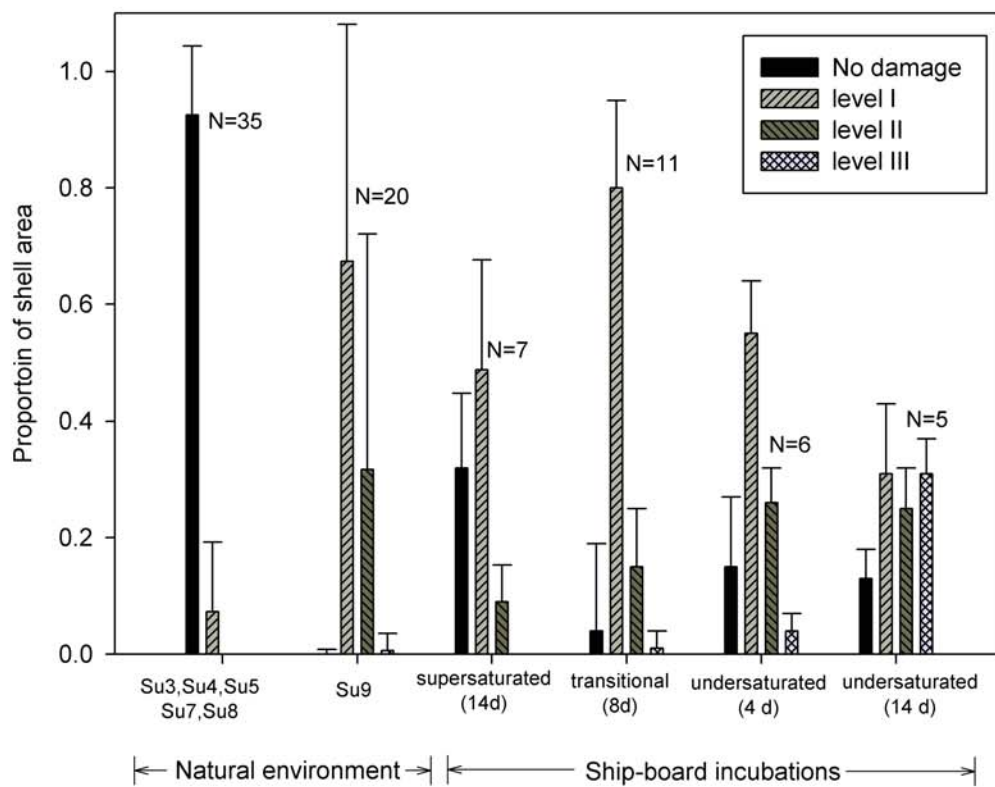
Supplementary Information:

Extensive dissolution of live pteropods in the Southern Ocean

Bednaršek N[1], Tarling GA[1]*, Bakker DCE[2], Fielding S[1], Jones EM[3], Venables HJ[1], Ward P[1], Kuzirian A[4], Lézé B[2], Feely RA[5], Murphy EJ[1]

*corresponding author: gant@bas.ac.uk

1. British Antarctic Survey, Natural Environment Research Council, Madingley Rd, Cambridge, CB3 0ET, UK
2. School of Environmental Sciences, University of East Anglia, Norwich Research Park, Norwich NR4 7TJ, UK
3. Royal Netherlands Institute for Sea Research, P.O. Box 59, 1790 AB Den Burg, Texel, The Netherlands
4. Department of Geology and Geophysics, Woods Hole Oceanographic Institution, Woods Hole, Massachusetts, USA
5. NOAA, Pacific Marine Environm Lab, Seattle, WA 98115 USA

Sensitivity study of the influence of anthropogenic carbon on surface water aragonite saturation state: To establish if anthropogenic CO_2 altered the carbonate chemistry at station Su9 (52.6°S, 39.1°W), a sensitivity study was conducted assuming that the changes in carbonate chemistry result only from the uptake of anthropogenic CO_2 while the ocean was temporarily invariant in all relevant water parameters, following the approach of Yamamoto-Kawai et al. (2009, Science 326:1098-1100).

An end-member mixing calculation was used to assess the extent of surface water mixing downwards. This was based on physical oceanographic measurements taken at Su9 (Venables et al. 2012, Deep-Sea Res II 59–60: 14–24). At this site, the winter mixed layer (WML) reached a maximum depth of 140 m, while unmodified Circumpolar Deep Water (CDW) reached a minimum depth of around 400 m (at which depth pCO_2 was 571 µatm). Using mixing rates calculated from the salinity profile, and not taking into account any further biological effects, the percentage ratio of WML to CDW water at 204 m (above which depth most pteropods were concentrated) was 58% to 42%. Dissolved inorganic carbon was assumed to mix conservatively following salinity mixing ratios. These calculations agreed with the penetration of CFCs below the mixed layer in data collected from the region on a separate research cruise (Brown, unpublished). Accordingly, the addition of 104 µatm of pCO_2 to surface waters resulting from anthropogenic CO_2 would reduce to 60.3 µatm at 204 m (and to 0 µatm at 400 m where there is no penetration of surface water).

The remaining carbonate chemistry parameters for present day and preindustrial situations were calculated using sysCO2 (http://cdiac.ornl.gov/ftp/cp2sys) for given input conditions of temperature, salinity, pressure and nutrient concentrations (Supplementary Tables 1 and 2). Comparison of the tables show that, in preindustrial conditions, Ω_A values at, for example, 182 m would have been above 1.167, as opposed to a present day value of 0.997.

Depth	Salinity	Phosphate	Silicate	Temp	TA	TC	pCO$_2$	pH_T	CARBONATE IONS			Omega aragonite
									CO$_2$	HCO$_3^-$	CO$_3^{2-}$	
(m)		(µmol kg^{-1})	(µmol kg^{-1})	(°C)	(µmol kg^{-1})	(µmol kg^{-1})	(µatm)		(µmol kg^{-1})			
82	33.91	1.82	28.56	1.24	2290.0	2165.2	385	8.044	23	2047	95	1.418
102	33.99	1.94	44.16	0.00	2286.9	2184.8	430	7.997	27	2075	82	1.220
121	34.03	1.99	49.14	-0.27	2287.4	2190.4	442	7.984	28	2083	80	1.174
142	34.10	2.07	55.57	-0.22	2295.7	2210.7	490	7.943	31	2106	74	1.081
162	34.18	2.14	61.12	0.10	2299.1	2213.4	496	7.938	31	2108	74	1.083
182	34.23	2.19	64.21	0.36	2301.2	2227.3	553	7.894	34	2125	68	0.997
203	34.31	2.24	68.44	0.73	2308.8	2234.2	563	7.888	34	2131	69	1.000
400	34.60	2.28	87.35	1.72	2336.8	2255.6	571	7.880	34	2149	73	1.014

Supplementary Table 1: Carbon chemistry parameters derived using Matlab CO2sys, total pH scale, Mehrbach refit by Dickson and Millero using measurements made at station Su9 (52.6ºS, 39.1ºW), Scotia Sea, Jan 2008.

Depth	Salinity	Phosphate	Silicate	Temp	TA	TC	pCO$_2$	pH_T	CARBONATE IONS			Omega arag-onite
									CO$_2$	HCO$_3^-$	CO$_3^{2-}$	
(m)		(µmol kg^{-1})	(µmol kg^{-1})	(°C)	(µmol kg^{-1})	(µmol kg^{-1})	(µatm)		(µmol kg^{-1})			
82	33.91	1.82	28.56	1.24	2290.0	2117.2	279	8.169	17	1978	123	1.825
102	33.99	1.94	44.16	0.00	2286.9	2145.5	324	8.108	20	2021	104	1.535
121	34.03	1.99	49.14	-0.27	2287.4	2153.0	336	8.092	21	2032	100	1.468
142	34.10	2.07	55.57	-0.22	2295.7	2178.5	384	8.040	24	2064	90	1.324
162	34.18	2.14	61.12	0.10	2299.1	2186.4	405	8.020	25	2073	88	1.285
182	34.23	2.19	64.21	0.36	2301.2	2203.5	459	7.969	28	2095	80	1.167
203	34.31	2.24	68.44	0.73	2308.8	2215.5	487	7.947	30	2108	78	1.132
400	34.60	2.28	87.35	1.72	2336.8	2255.6	571	7.880	34	2149	73	1.014

Supplementary Table 2: Carbon chemistry parameters derived using Matlab CO2sys, total pH scale, Mehrbach refit by Dickson and Millero using measurements made at station Su9 (52.6ºS, 39.1ºW), Scotia Sea, Jan 2008, but assuming preindustrial atmospheric pCO$_2$ levels.
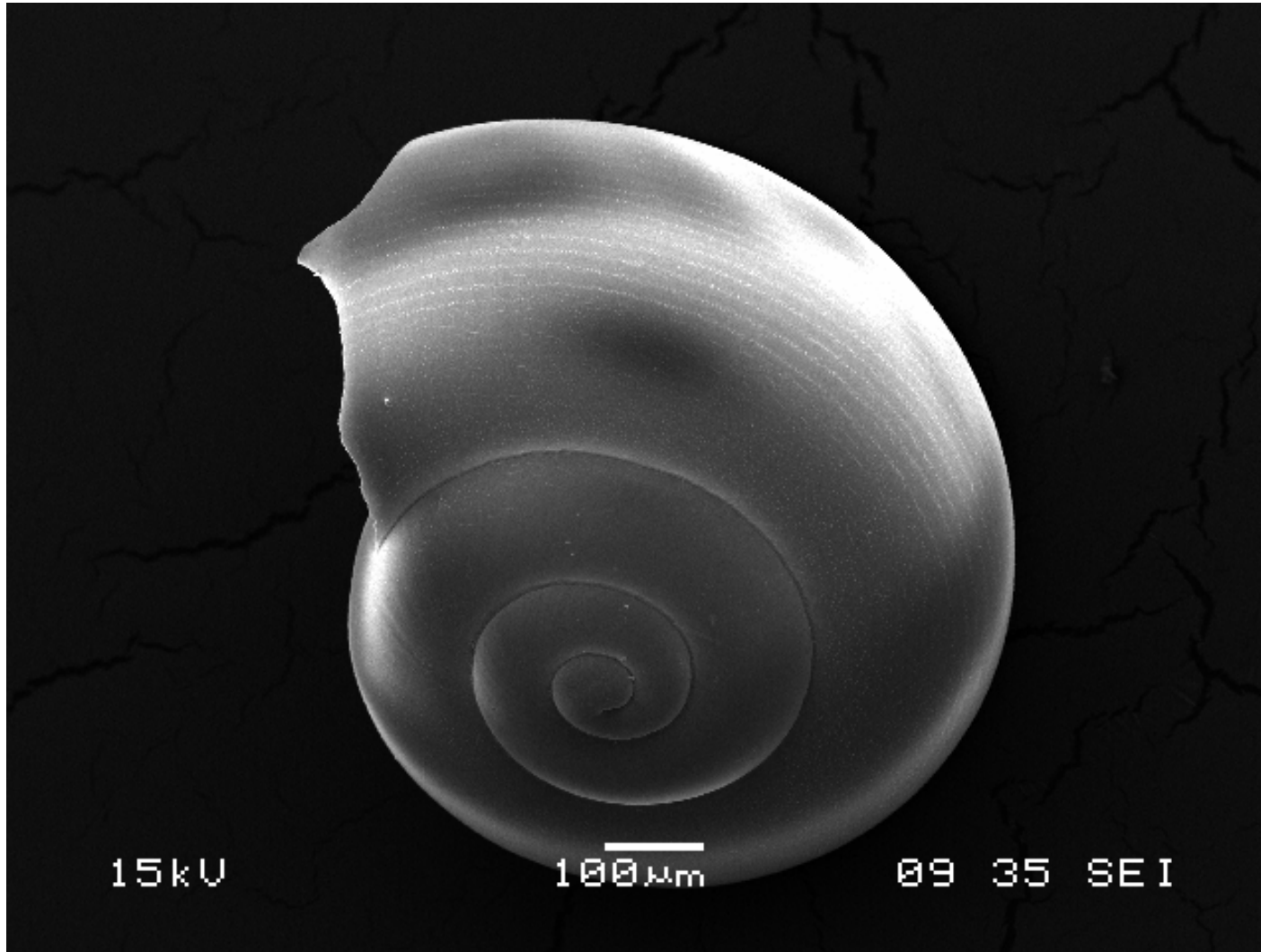
Supplementary Figure 1. High resolution SEM images of juvenile *Limacina helicina antarctica* showing intact animal without any indications of dissolution.
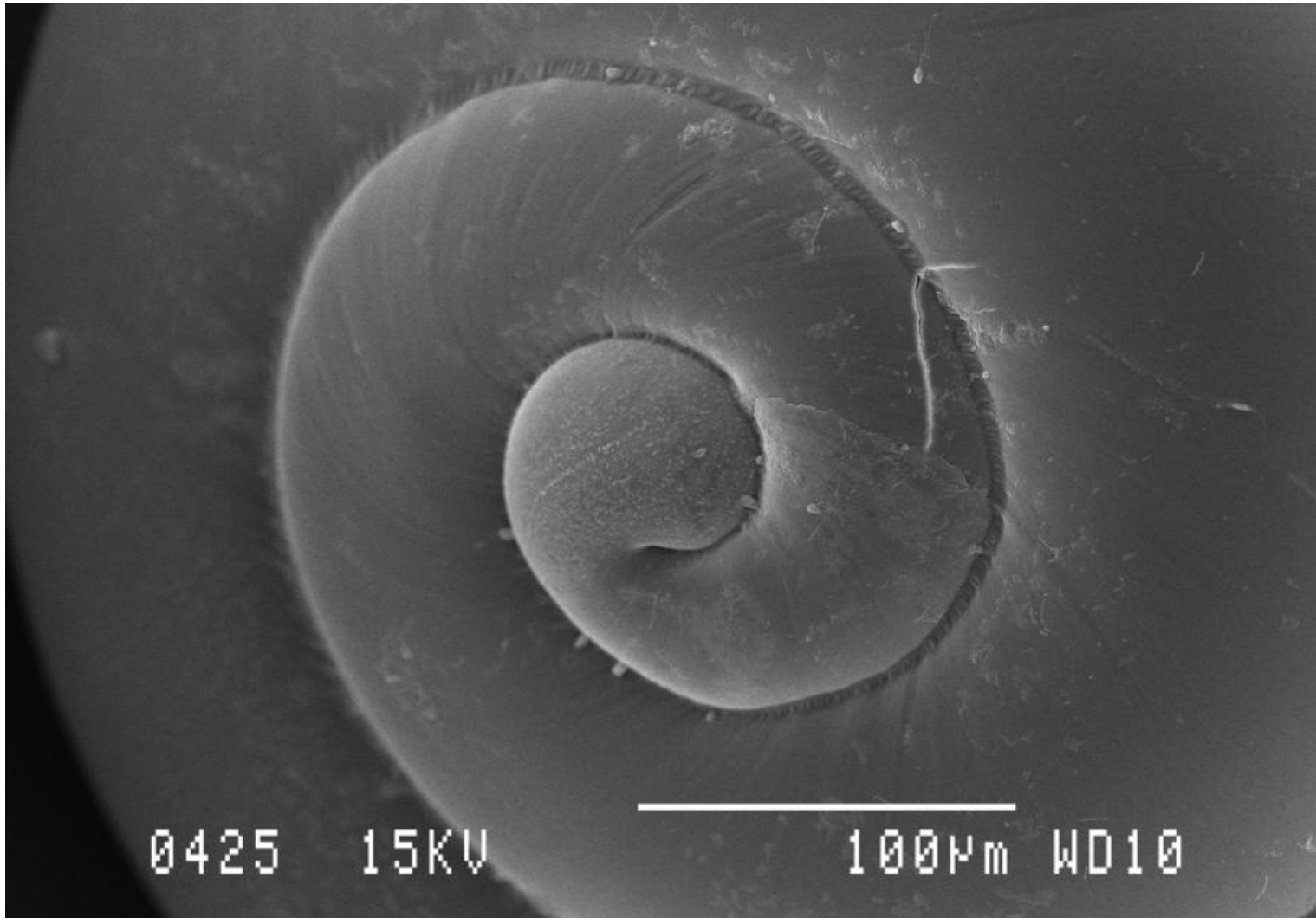
Supplementary Figure 2. High resolution SEM images of juvenile *Limacina helicina antarctica* showing intact animal without any indications of dissolution.
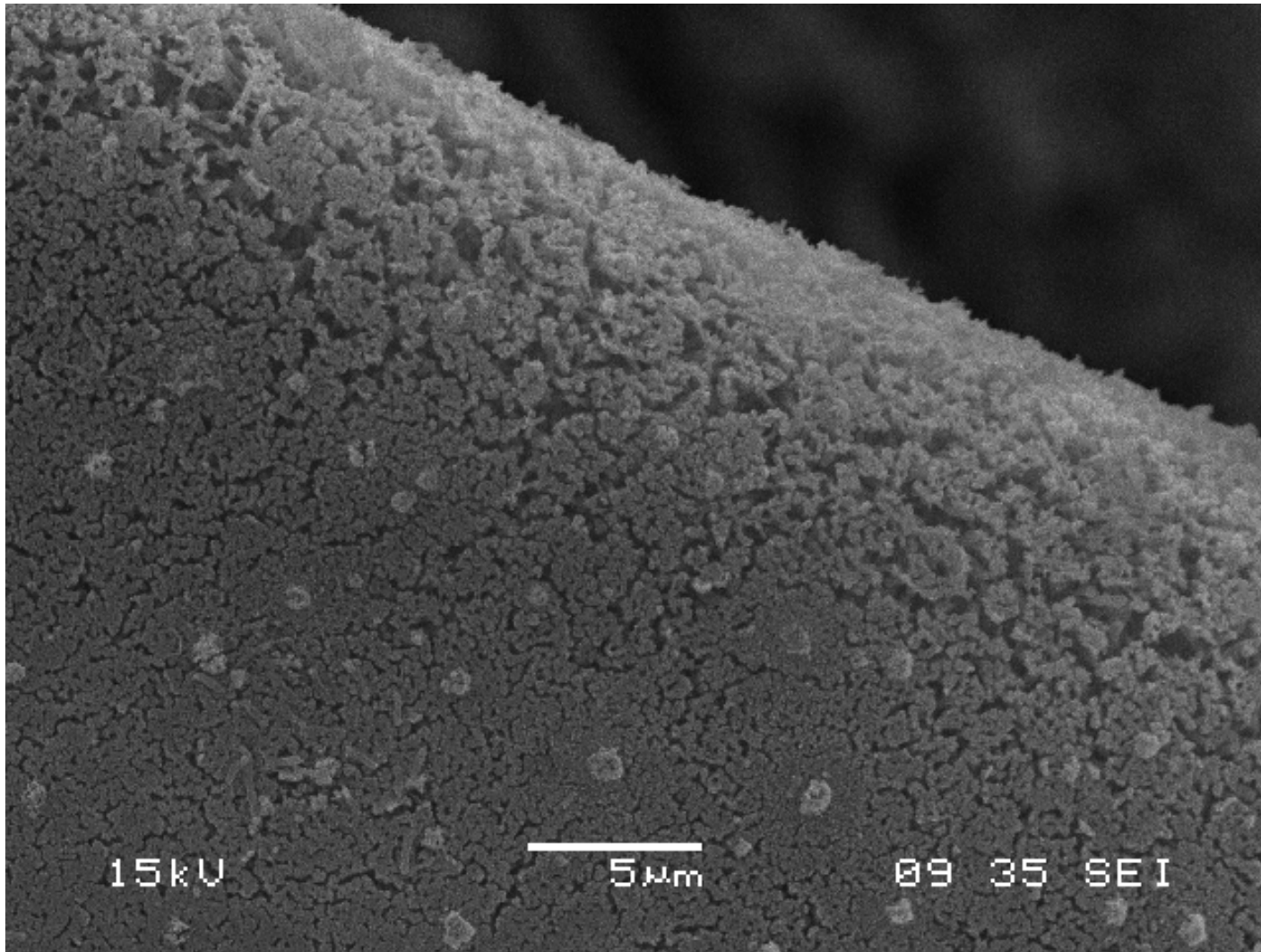
Supplementary Figure 3. High resolution SEM images of juvenile *Limacina helicina antarctica* showing level I dissolution: the upper prismatic layer slightly dissolved.
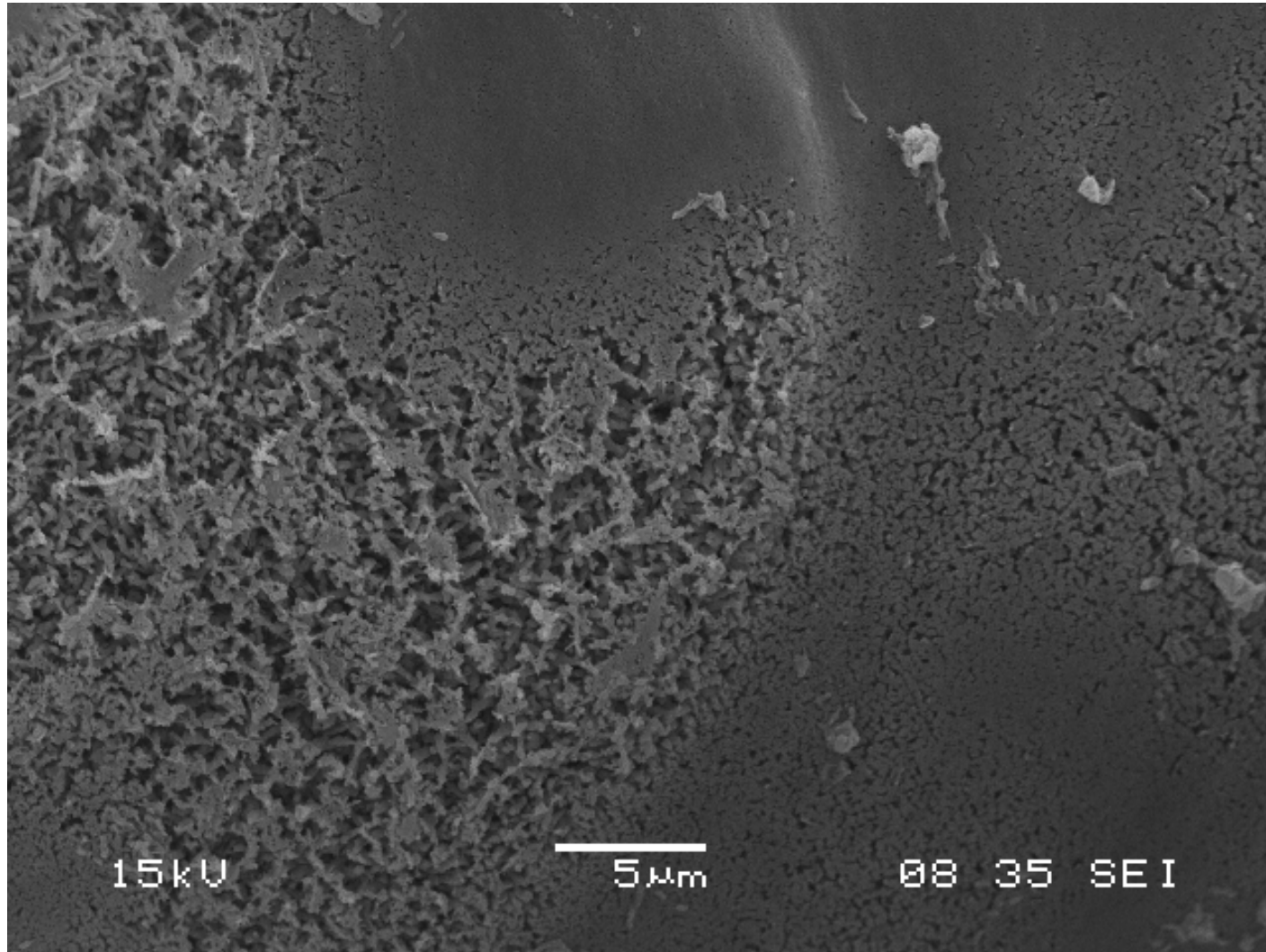
Supplementary Figure 4. High resolution SEM images of juvenile *Limacina helicina antarctica* showing level II dissolution: the prismatic layer partially or completely missing and the cross-lamellar matrix partially exposed with increasing porosity in the upper crystalline layer.
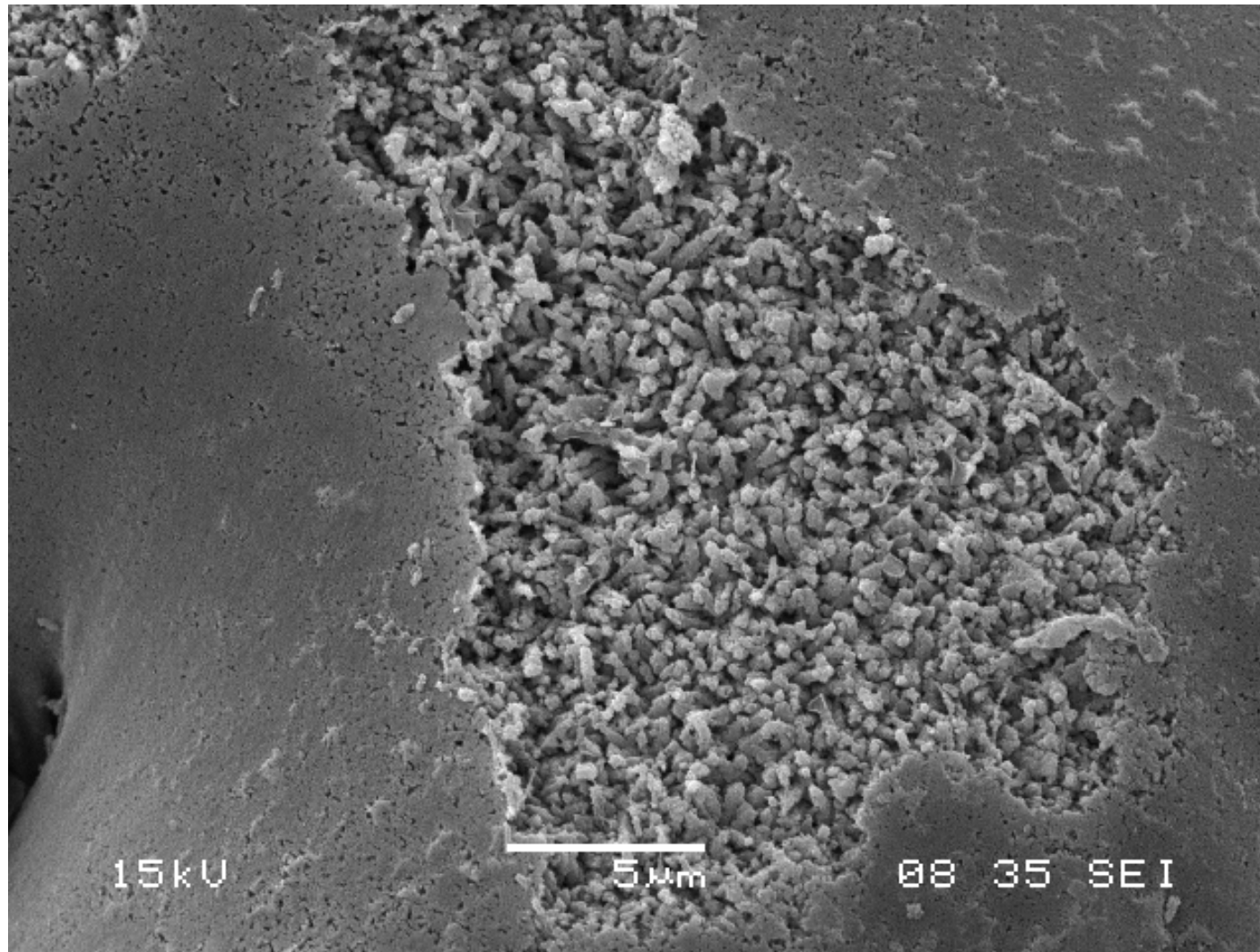
Supplementary Figure 5. High resolution SEM images of juvenile *Limacina helicina antarctica* showing level III dissolution: the crossed-lamellar matrix showing signs of dissolution across large areas of the shell, the shell becoming more fragile due to fragmentation. Crystals transform from elongated rods to being more 'cauliflower-like' in appearance.
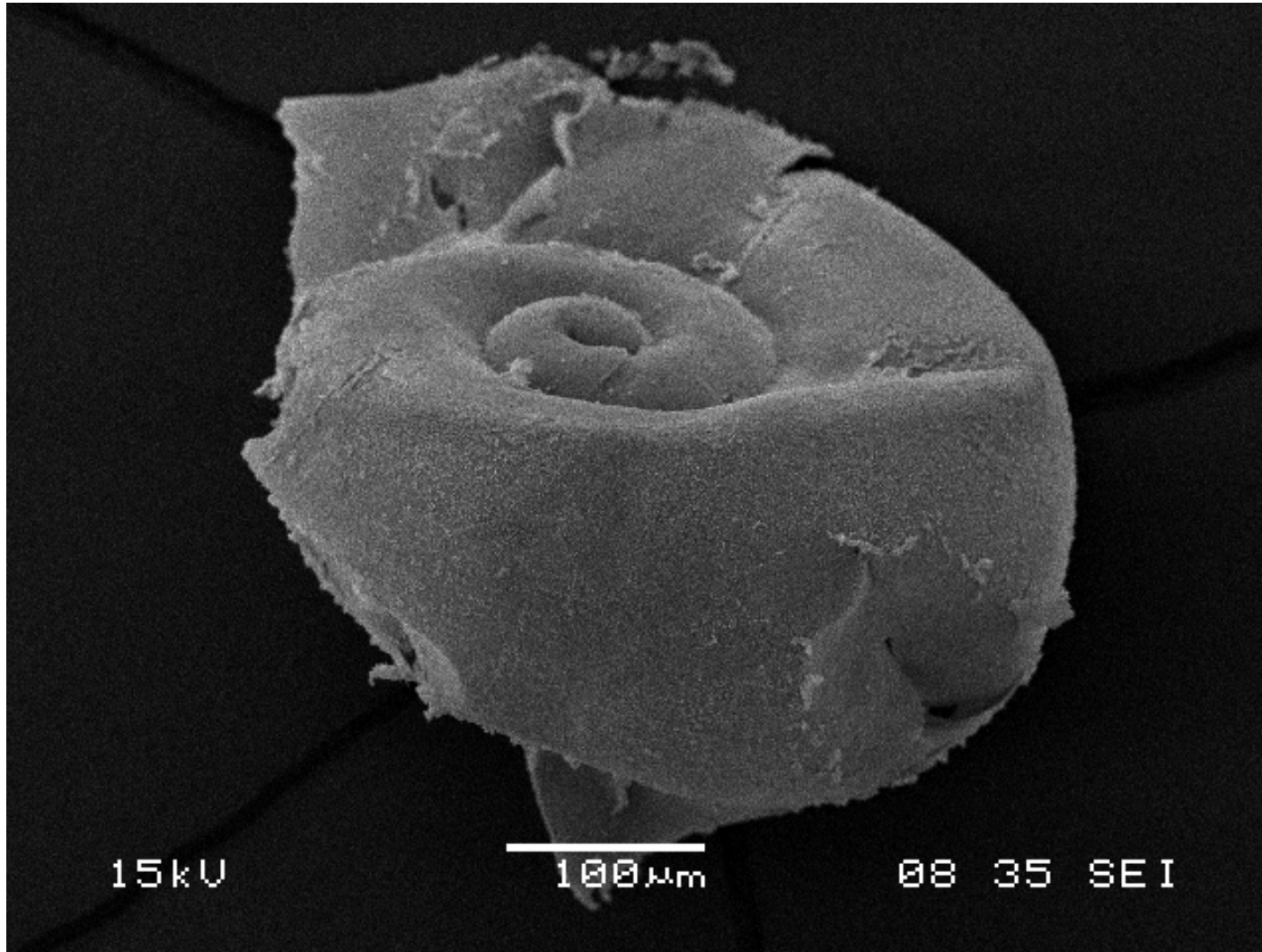
Supplementary Figure 6. High resolution SEM images of juvenile *Limacina helicina antarctica* showing level III dissolution: the crossed-lamellar matrix showing signs of dissolution across large areas of the shell, the shell becoming more fragile due to fragmentation.